Note

Rapid microwave-assisted synthesis of saponites and their use as oxidation catalysts

R. Trujillano [a,*], E. Rico [a], M.A. Vicente [a], V. Rives [a], K.J. Ciuffi [b], A. Cestari [b], A. Gil [c], S.A. Korili [c]

[a] GIR-QUESCAT, Departamento de Química Inorgánica, Universidad de Salamanca, Plaza de la Merced S/N, 37008 Salamanca, Spain
[b] Universidade de Franca, Av. Dr. Armando Salles Oliveira, 201 Pq. Universitário CEP 14404600 Franca, Sao Paulo, Brazil
[c] Departamento de Química Aplicada, Universidad Pública de Navarra, Pamplona, Spain

ARTICLE INFO

ABSTRACT

Saponites containing divalent Mg, Ni, or Fe as octahedral cations and trivalent Al and Fe substituting Si in the tetrahedral sheet were synthesized using microwave radiation. Saponite with a high specific surface area was obtained in all the syntheses, although Fe-Al saponite crystallized was impurified by Fe_2O_3 and analcime. The catalytic activity of the solids for the epoxidation of (Z)-cyclooctene by hydrogen peroxide was tested, the solids obtained being highly active (conversion up to 8.8%, and 100% selectivity to the epoxide).

© 2010 Elsevier B.V. All rights reserved.

1. Introduction

Synthetic saponites have been widely studied because of their potential application as catalysts or catalyst supports (Carniato et al., 2009; Kshirsagar et al., 2009a,b; Polverejan et al., 2002; Trujillano et al., 2009; Zhang et al., 2010; Zhou, 2010). These smectitic clays, with a cell theoretical formula of $[Si_{8-x}Al_x]^t$ $[M_6^{2+}]^o$ O_{20} $(OH)_4$ $[M_x^+]\cdot nH_2O$, exist in nature as a magnesic–ferrous solid solution. When $M^{2+} = Mg$, the resulting mineral is called saponite proper; when $M^{2+} = Fe$, the mineral is known as ferrous saponite. Although natural mineral clays are cheap and readily available, disadvantages such as the presence of mineral impurities, the long and tedious purification procedures, and the heterogeneity of the resulting solids have led industries to turn to the use of synthetic clays. The synthesis of saponite avoids the problems related to the presence of impurities, once pure samples have been obtained. Moreover, saponites with a fixed chemical composition, textural properties, and cation exchange capacity, among other characteristics, can be achieved by synthetic means. However, the preparation of synthetic clays is not straightforward, and several routes that usually require hydrothermal synthesis at high temperatures and pressures have been proposed, (Bisio et al., 2008; Bosbach et al., 2009; Higashi et al., 2007; Kawi and Yao, 1999; Kloprogge et al., 1993, 1999; Prihod'ko et al., 2002, 2004; Trujillano et al., 2009).

Microwave heating has recently been reported as an alternative approach for the synthesis of saponites, since shorter reaction times

and lower temperatures can be employed. Furthermore, microwave treatment is faster, cleaner, and often more efficient than conventional heating, because microwave energy can be transformed directly into heat in the bulk of the dielectric materials, where it is then absorbed and transferred by different absorption mechanisms such as dipolar relaxation or ion conduction. Zemanová et al. (2006) have used microwave radiation to modify the layer charge of smectites. In fact, microwaves have found countless applications in the field of clay materials chemistry, such as the production of pillared clays (Sivaiah et al., 2010) and the ageing of layered double hydroxides (Benito et al., 2009, 2010; Herrero et al., 2009). To our knowledge, only a few works in the literature have reported the direct synthesis of saponite-like materials by means of microwave radiation (Trujillano et al., 2010; Vicente et al., 2010; Yao et al., 2005), and the application of these materials in catalysis has not yet been reported. Thus, the present paper describes the synthesis of saponites containing different cations in the octahedral and tetrahedral layers by microwave radiation and reports the use of the resulting materials as catalysts for the epoxidation of (Z)-cyclooctene by hydrogen peroxide.

2. Experimental

2.1. Synthesis

A commercial sodium silicate aqueous solution ($SiO_2.NaOH$, SiO_2 27 wt.%, density 1.39 g/mL, Aldrich) was added to another solution prepared by the dissolution of 3.60 g NaOH and 6.56 g $NaHCO_3$ in 50 mL of distilled water. Then, 5.0 mL of an aqueous solution containing stoichiometric amounts of the chlorides of the divalent and trivalent cations at the desired ratios was slowly added to the

---

resulting mixture under continuous and vigorous stirring. The saponite formula targeted by us was $[Si_7M^{III}_1]$ $[M^{II}_6]$ O_{20} $(OH)_4$ $[Na_1] \cdot nH_2O$, where $M^{III} = Al^{3+}$ or Fe^{3+}, and $M^{II} = Mg^{2+}$, Ni^{2+}, or Fe^{2+} (in one of the samples, half of the stoichiometric divalent cations consisted of Mg^{2+} and the other half comprised Ni^{2+}). Thus, the following molar ratios were considered: $Si/M^{III} = 7{:}1$ and $Si/M^{II} = 7{:}6$. The gels obtained were sealed in a 100-mL Teflon reactor and were treated hydrothermally in a Milestone Ethos Plus microwave furnace at 180 °C, for 8 h. Six different saponites were obtained. The resulting materials were labeled $M^{II}M^{III}$ to indicate the presence of the divalent and trivalent cations employed in the synthesis (see Table 1).

2.2. Characterization techniques

Chemical analysis of the elements present in the materials was carried out by atomic absorption spectroscopy in a Perkin Elmer Elan 6000 ICP Mass Spectra apparatus at the Servicio General de Análisis Químico Aplicado (University of Salamanca, Spain). The X-ray powder diffraction (XRPD) patterns were recorded on a Siemens D-500 diffractometer equipped with the Diffract-AT software and a DACO-MP microprocessor, a copper anode ($\lambda = 1.5405$ Å), and a graphite filter. The FT-IR spectra were acquired on a Perkin Elmer FT-IR-1600 spectrometer in the 4000 to 400 cm^{-1} range, using the KBr pellet technique. Nitrogen (L'Air Liquide, Spain) adsorption–desorption isotherms at −196 °C were obtained on a Micromeritics Gemini instrument, after degassing the samples for 2 h at 110 °C in a Micromeritics Flowprep 060 device. Specific surface area and external surface area values were calculated by means of the BET and the t-plot methods, respectively, and the micropore volume was estimated from the amount of nitrogen adsorbed at $p/p^o = 0.95$. Diffuse reflectance UV–Vis (RD-UV–Vis) spectra were recorded in the 300–1100 nm range on a Perkin-Elmer Lambda 35 spectrophotometer equipped with a Labsphere RSA-PE-20 integration sphere, connected to a PC operating with the UV WinLab 2.85 software, using a slit width of 2 nm and MgO as reference.

2.3. Catalytic performance

The epoxidation of (Z)-cyclooctene by hydrogen peroxide was selected for evaluation of the catalytic behavior of the synthetic saponites. Hydrogen peroxide (1.28 mmoL) 30 or 70 wt.% H_2O_2, used as received, was added to a 4-mL vial sealed with a Teflon-coated silicone septum containing the catalyst (10 mg), a 1:1 1,2-dichloro-ethane/acetonitrile solvent mixture (1 mL), (Z)-cyclooctene (previously purified on an alumina column) as substrate (1.15 mmol), and cyclohexanone as internal standard (10 μL).

The reactions were performed at atmospheric pressure and room temperature. The reaction progress was monitored by gas chromatography on an HP 6890 chromatograph equipped with a hydrogen flame ionization detector and an HP-INNOWax capillary column (length of 30 m, internal diameter of 0.25 μm). The products were determined on the basis of their retention times as compared with the authentic samples; cyclohexanone was employed as the internal standard. Two blank tests were also carried out. The first was accomplished in the presence of hydrogen peroxide but in the absence of catalyst; the second was conducted in the presence of a saponite catalyst but without the addition of hydrogen peroxide. The results are expressed in terms of cyclooctene conversion, since selectivity was always 100% for the corresponding oxide, namely cyloocteneoxide. The unreacted hydrogen peroxide was determined by iodometric titration.

3. Results and discussion

3.1. Physicochemical characterization

The chemical analysis data for Si, Na, Al, Mg, Ni, and Fe are given as the percentage contents of the corresponding oxides, allowing calculation of the corresponding formulae (Table 1). The water content was estimated by difference, since no other volatile compounds were present in the solids.

The structural formula obtained for some of the compounds synthesized here was very close to the theoretical one, particularly in the case of the samples NiMgAl, NiFe, and MgFe samples. This is in agreement with the presence only of the saponite phase, as revealed by the X-ray diffractograms (see below). Regarding the NiAl and MgAl samples, there was an excess of the divalent element with respect to the expected value, although no other phases were detected in the X-ray diffractograms. Thus, even though saponite was the predominant phase in these two samples, there might have been co-precipitation of a certain amount of the divalent element as the corresponding hydroxide. Finally, the structural formula of the sample FeAl was not calculated because the presence of other crystalline phases (see below) would render such a formula meaningless.

In most cases, there was good agreement between the obtained and theoretical formulae for all the parameters. Thus, the degree of substitution of Si by M^{III} in the tetrahedral sites was close to the targeted value of 1.00 for all the samples except MgAl, for which the degree of substitution was higher, even too high for a saponite. The fact that Si substitution occurred even more easily when the trivalent cation was Al^{3+}, compared with Fe^{3+}, is remarkable. This, together with the excess Mg (in the formula as $Mg(OH)_2$) in MgAl, suggests the presence of an additional phase that probably consists of Mg and Al, although it was not detected by XRPD. The degree of occupancy of the octahedral sites was always very high and was complete in several cases, as expected for saponites (it is noteworthy that nearly all the layer charge in natural saponites originates from Si-Al substitutions in the tetrahedral layer, while the octahedral layer is almost or completely occupied). Consequently, the charge balances were very good for all the samples. The theoretical Cation Exchange Capacity (CEC) of these samples ranged between 0.50 and 0.82 meq/g, as calculated from the amount of exchangeable cations and the "molecular mass" of each solid.

Table 1
Chemical analysis (%), textural properties, and catalytic activity in the epoxidation of Z-cyclooctene of the prepared solids.

Sample	Chemical analyses								Textural analyses			Catalytic activity		
	SiO_2	Al_2O_3	Fe_2O_3	NiO	MgO	Na_2O	H_2O	Formula	S_{BET} (m²/g)	S_t (m²/g)	V_m (cm³/g)	C_{24} (%)	C_{48} (%)	S (%)
NiAl	25.09	3.14	–	35.63	–	1.48	34.66	$[Si_{6.97} Al_{1.03}][Ni_{6.00}]O_{20}(OH)_4[Na_{0.80}] \cdot 28H_2O$ 1.35 $Ni(OH)_2$	201	152	0.028	6.2	7.0	100
NiMgAl	33.23	4.01	–	19.22	9.40	2.06	32.08	$[Si_{6.96}Al_{0.99}][Ni_{3.24} Mg_{2.76}]O_{20}(OH)_4[Na_{0.84} Mg_{0.09}] \cdot 20H_2O$	334	269	0.039	6.4	8.8	100
MgFe	44.23	–	7.74	–	23.98	2.23	21.82	$[Si_{7.20} Fe_{0.80}][Mg_{5.82}Fe_{0.15}]O_{20}(OH)_4[Na_{0.70}] \cdot 10H_2O$	467	375	0.055	7.3	7.5	100
NiFe	34.30	–	6.42	34.74	–	2.01	22.53	$[Si_{7.14} Fe_{0.86}][Ni_{5.81}Fe_{0.14}]O_{20}(OH)_4[Na_{0.81}] \cdot 14H_2O$	217	166	0.029	5.6	5.6	100
FeAl	33.26	4.08	45.45	–	–	5.79	11.16		–	–	–	4.8	4.9	100
MgAl	21.72	4.82	–	–	22.79	2.59	48.08	$[Si_{6.34}Al_{1.66}][Mg_{6.00}]O_{20}(OH)_4[Na_{1.46} Mg_{0.10}] \cdot 34H_2O \cdot 3.83 Mg(OH)_2$	366	315	0.029	4.7	4.8	100

S_{BET} = Specific surface area, S_t = External surface area, V_m = Micropore volume, C_{24} = Conversion after 24 h, C_{48} = Conversion after 48 h, S = Selectivity to cyclooctenoxide.

The diffraction patterns of the samples synthesized were similar to those of saponite, and the *d* spacings coincided with those of raw saponites (Fig. 1). An important reflection signal for the characterization of this type of clay is the one close to 61° (2θ), usually indexed as (06,33). This reflection does not depend on the *c*-axis and is related to the *b* parameter of the cell, allowing a distinction to be made between dioctahedral and trioctahedral clays. This reflection was recorded at 1.52 Å for all the samples synthesized here, demonstrating their strong trioctahedral character (Prihod'ko et al., 2004). The other in-plane reflections were also clearly identified, confirming that saponite layers existed in all the samples, although the stacking of these layers along the *c*-axis (00l reflections) varied considerably among the solids.

The (001) reflection detected for the NiAl, NiFe, and FeAl samples was well defined, and the basal spacings were 15.3, 15.7, and 12.1 Å, respectively. Besides the characteristic saponite peaks, peaks due to Fe_2O_3 and analcime (a silicate with a formula of $NaAlSi_2O_6 \cdot H_2O$) were also recorded in the case of the FeAl sample. For this reason, FeAl was not further characterized, although its catalytic activity was evaluated. The MgAl sample exhibited a low degree of ordering along the *c*-axis (d ~15.4 Å), a value that was even lower for the NiMgAl sample. This indicates that there is no long-range ordering of the layers along the *c*-axis. Regarding the MgFe sample, the layers were not stacked at all along this axis. Considering the divalent cations tested here, it is evident that the presence of Ni favors *c*-ordering as compared with Mg and Fe. This was rather surprising, since due to its natural abundance Mg is the major octahedral cation found in raw saponites. Nevertheless, it was evident that the high affinity of Ni^{2+} for the octahedral positions of the clay structure strongly favored the synthesis of saponite. In respect to the trivalent cations, solids containing Al were better ordered than those containing Fe. The latter effect was not unexpected, since Al is the element that usually substitutes Si in the tetrahedral sheet of clays.

The FT-IR spectra of the solids (Fig. 2) were also typical of saponites. The band around 3450 cm^{-1} was due to the stretching mode of adsorbed water molecules, whose bending mode was recorded at 1642 cm^{-1}. The shoulder around 3220 cm^{-1} can be ascribed to the O-H stretching mode of H-bridged OH groups, while the M(II)-O-H stretching vibration at higher wavenumbers denotes the trioctahedral character of synthetic saponites (Madejová, 2003). The latter band was very sensitive to the nature of the divalent cations present in the octahedral sites. Indeed, it was recorded at 3687, 3632, and 3548 cm^{-1} for the samples containing Mg^{2+}, Ni^{2+}, and Fe^{2+}, respectively.

Fig. 2. FT-IR spectra of the samples indicated.

The lattice vibration bands were recorded close to 1015, 708–670, and 465 cm^{-1} and can be assigned to the Si-O-Si, M(II)-OH stretching, and Si-O-M(II) bending modes, respectively. In raw saponites, the shoulder at 795 cm^{-1} has usually been attributed to the presence of small amounts of amorphous SiO_2. The band at 420 cm^{-1} has also been ascribed to the presence of SiO_2 (Kloprogge and Frost, 2000).

The UV–Vis spectra of the solids containing Ni^{2+} – that is, NiAl, NiMgAl, and NiFe (Fig. 3) – corroborated the presence of octahedrally coordinated Ni^{2+} (Sutton, 1970). The positions of the bands as well as the transitions they corresponded to are summarized in Table 2, where the bands recorded for the precursor salt, $NiCl_2 \cdot 6H_2O$, have also been included. The bands recorded for saponites were shifted toward higher energy values than those of the precursor salt. This is expected because of the different ligands surrounding Ni^{2+} in both cases (Wells, 1984).

Concerning $NiCl_2 \cdot 6H_2O$, the band corresponding to the first transition was not detected in its UV–Vis spectrum because it appeared in the near infrared (NIR) region. For the synthesized saponites, this band appeared at about 1100 nm (~9100 cm^{-1}). In contrast, the third band overlapped with the charge transfer band, mainly in the case of the saponite solids (~395 nm). The band due to the second spin-allowed transition split into two maxima due to the spin-orbit coupling. All these bands are characteristics of Ni^{2+} in an octahedral environment.

The nitrogen adsorption–desorption isotherms of the synthesized samples displayed a similar shape (Fig. 4). They belonged to type I,
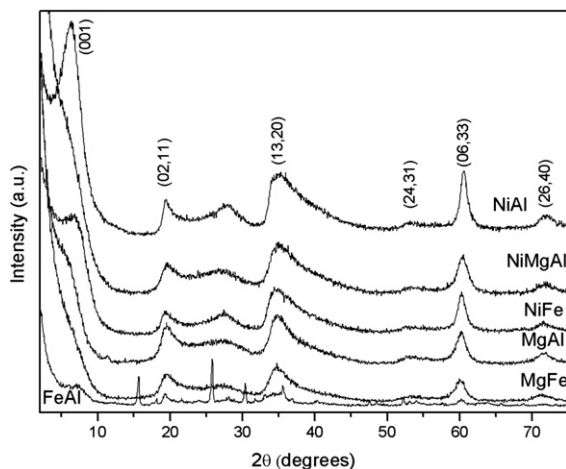

Fig. 1. X-ray diffraction patterns of the samples indicated, with indexation of the peaks from saponite. The acute peaks in FeAl sample diffractogram correspond to Fe_2O_3 and analcime.
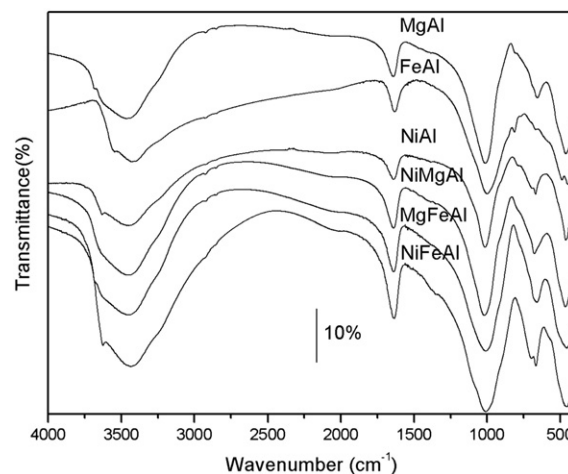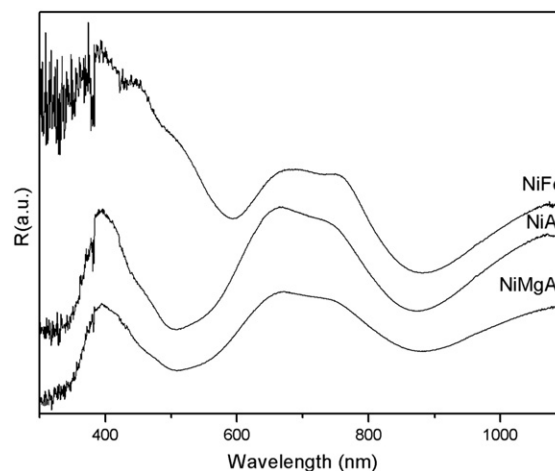

Fig. 3. RD-Visible spectra of the indicated Ni-containing saponites.

Table 2
Electronic transitions for the synthesized saponites and for the precursor $NiCl_2 \cdot 6H_2O$.

Electronic transitions	$^3A_{2g}$ (F) → $^3T_{2g}$ (F)	$^3A_{2g}$ (F) → $^3T_{1g}$ (F)	$^3A_{2g}$ (F) → $^3T_{1g}$ (P)
$NiCl_2 \cdot 6H_2O$	–	690,770	413
Saponites	~1100	663,750	394

which is typical of microporous powders where adsorption is limited to only a few molecular layers. All isotherms presented type E hysteresis loops, in which the desorption branches exhibited a small slope at high relative pressures (Lowell, 1979). The specific surface areas calculated by the BET method lay between 217–467 m²/g. These values were considerably higher than those usually reported for raw saponites. We have recently related the high specific surface area of microwave-synthesized saponites to their particle size, which strongly depends on the synthesis conditions (Trujillano et al., 2010). It should be noted that the specific surface area of Ni-saponites was lower than that of Mg-saponites, which is in agreement with the better c-axis ordering of the Ni-samples. In other words, solids with a low degree of layer stacking along the c-axis display high specific surface area values. This is expected owing to the easier access of the adsorbate to the surface of these "independent" layers. The probable presence of small amounts of amorphous phases in the Mg-samples may also account for their larger specific surface areas.

The t-plots obtained for the synthesized samples (Fig. 5) afforded straight lines which, after extrapolation to the low relative pressure region, gave a positive zero-intercept. The external surface areas were also very high, between 152–375 m²/g, amounting to ca. 80% of the total surface area. Micropore volumes varied in the 0.028–0.055 cm³/g range, whereas micropore surface areas lay between 49–92 m²/g. The downward deviation from the straight line at t values larger than 6 Å suggests that narrow pores were filled by multilayer adsorption at low relative pressures, thereby reducing the surface available for continued adsorption (Lowell, 1979).

3.2. Catalytic activity

All the saponite samples synthesized in this work were tested as catalysts for the epoxidation of cis-cyclooctene, and the results are depicted in Table 1. Initial tests were carried out using 30 wt.% H_2O_2 as oxidant, but the conversion of cis-cyclooctene was low (c.a. 1% after 48 h), as previously described in a work reporting the catalytic activity of synthetic Ni(II) or Mg(II) saponites prepared by hydrothermal synthesis (Trujillano et al., 2009). This result can be attributed to the degradation of hydrogen peroxide under the reaction conditions
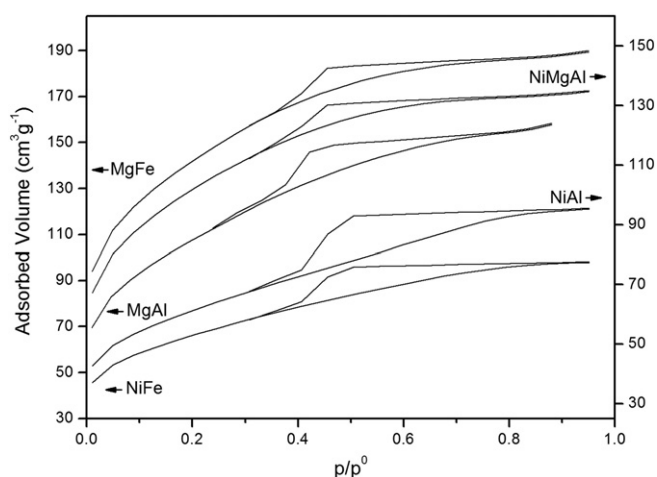

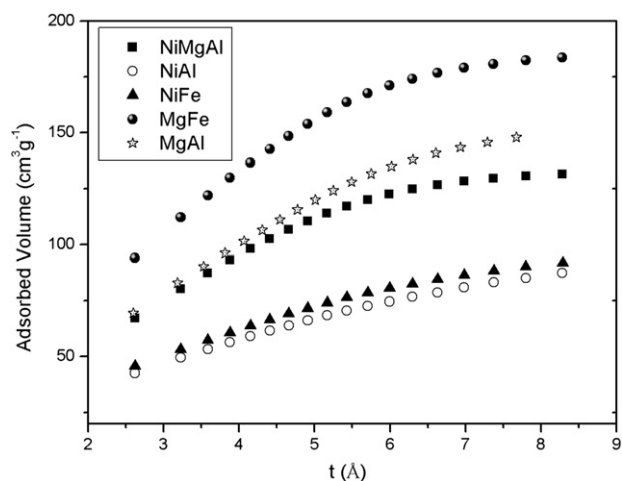Fig. 4. Nitrogen adsorption-desorption isotherms of the samples indicated.

Fig. 5. t-plots of the samples indicated.

employed, with subsequent catalyst deactivation due to the presence of water. To avoid this problem, the reactions were performed using 70 wt.% H_2O_2 as oxidant. According to the literature (Rinaldi et al., 2004), the use of 70 wt.% H_2O_2 improves the lifetime and productivity of the catalyst because of the limited extent of hydrogen peroxide decomposition. Thus, only the results obtained with 70 wt.% H_2O_2 are given in Table 1.

All the samples synthesized efficiently catalyzed the epoxidation of Z-cyclooctene, with cyclooctene conversions between 4.7 and 8.8%. It is noteworthy that the only oxidation product was cyclooctene epoxide, which was produced with 100% selectivity under all experimental conditions and during all the reaction times tested, without the formation of by-products. In the case of the NiAl and NiMgAl samples, conversion increased noticeably from 24 to 48 h, while for the other samples conversion was almost constant, or slightly increased. Maximum conversions were obtained for the MgFe and NiMgAl samples after 48 h of reaction. Although the catalytic activity of Mg may seem surprising, we have recently reported that this cation plays an essential role in the Baeyer–Villiger reaction catalyzed by a synthetic saponite (Trujillano et al., 2009).

The consumption of hydrogen peroxide was very high for all the solids: ca. 94% after 48 h of reaction. This may be attributed to the decomposition of hydrogen peroxide induced by the acid centers of the catalysts. Indeed, saponites contain a large concentration of these centers because of the high degree of Si-Al substitution in the tetrahedral sites. In order to verify this point, a blank test was carried out by adding cyclooctene, hydrogen peroxide, and the solvent to the reaction vessel in the absence of any catalyst. After 48 h, all the initial hydrogen peroxide remained unreacted, unequivocally showing that its decomposition during the catalytic reactions had been induced by the studied catalysts.

The MgFe and NiMgAl solids furnished the best catalytic results. This was somewhat puzzling, because other solids containing Mg^{2+} or Ni^{2+} in octahedral sites afforded lower conversions. Moreover, regarding the tetrahedral sites, the presence of Al^{3+} and Fe^{3+} did not indicate a clear trend in the catalytic activity. Although the two solids with the highest conversion values had large specific surface areas, this magnitude was not decisive. For instance, the MgAl sample, also with a large specific surface area, displayed low catalytic activity, and the opposite was the case of the NiAl sample. Apart from the composition and textural properties, another factor that can influence the catalytic behavior of saponites is acidity. How acid a saponite is depends mainly on the degree of Si-M(III) substitution in the tetrahedral sheet, as well as on the nature of the divalent cation in the vicinity of the tetrahedra. Again, no clear trends were evident in the group of solids compared here. Therefore, it seems that their catalytic activity was influenced by a combination of all these factors.

Since no oxidation product was detected in the blank tests carried out in the absence of the samples prepared in this work, it is evident that the metal cations present in the saponites synthesized here catalyzed the reaction, and that hydrogen peroxide was the oxidant. The cations present in the prepared materials were responsible for the formation of the active species that transferred the oxygen atoms to the substrate. The fact that the NiMgAl sample provided the highest conversion percentages suggests that a synergistic effect takes place when two different cations are present in adjacent octahedral positions. However, further tests using samples with these characteristics are necessary to confirm this effect.

It is important to note that these preliminary results are very promising because the metal ions are located in the octahedral layers of the material, which hinders the access of the substrate to the active sites of the catalysts. In fact, the results obtained here are fairly similar to those achieved with a natural saponite impregnated with Ni-salts (Mata et al., 2009), with the advantage that the preparation of synthetic saponites by microwave radiation is a much faster method, thereby eliminating lengthy preparations and tedious purification procedures. Furthermore, the location of the active cations in the octahedral positions of the saponite might also be advantageous, since this may stabilize the catalyst. Indeed, it is noteworthy that there was no leaching of the metallic cations from the samples during the catalysis experiments, which also implies that the catalytic process was truly heterogeneous in all cases.

When hydrogen peroxide is employed as oxidant, radical species may be generated via its homolytic cleavage. To check whether radical mechanisms were involved in these synthetic saponites, the reactions were accomplished in the presence of *tert*-butyl alcohol. This radical scavenger did not diminish substrate conversion, such that the involvement of radical species as oxidizing agents can be ruled out.

These catalytic data lead to the conclusion that microwave synthesis enables the preparation of selective catalytic materials. Further studies involving solids with different chemical compositions and tetrahedral substitutions may shed light on the behavior of these catalysts.

4. Conclusions

The solids synthesized in the present work had the structure of saponite, as demonstrated by the XRPD and FT-IR data, although the FeAl sample consisted of saponite crystallized with other phases. The UV–Vis spectra of the samples containing nickel revealed that the Ni^{2+} cations were always located in octahedral sites. The specific surface area of the samples was large enough to allow their use as solid catalysts. The results from the epoxidation of (Z)-cyclooctene by hydrogen peroxide confirmed that the synthetic method was extremely satisfactory and that it afforded saponites able to act as good oxidation catalysts.

Acknowledgements

References

Benito, P., Herrero, M., Labajos, F.M., Rives, V., 2010. Effect of post-synthesis microwave–hydrothermal treatment on the properties of layered double hydroxides and related materials. Appl. Clay Sci. 48, 218–227.

Benito, P., Labajos, F.M., Rives, V., 2009. Microwaves and layered double hydroxides: a smooth understanding. Pure Appl. Chem. 81, 1459–1471.

Bisio, C., Gatti, G., Boccaleri, E., Marchese, L., Superti, G.B., Pastore, H.O., Thommes, M., 2008. Understanding physico-chemical properties of saponite synthetic clays. Microporous Mesoporous Mater. 107, 90–101.

Bosbach, D., Luckscheiter, B., Brendebach, B., Denecke, M.A., Finck, N., 2009. High level nuclear waste glass corrosion in synthetic clay pore solution and retention of actinides in secondary phases. J. Nucl. Mater. 385, 456–460.

Carniato, F., Bisio, C., Gatti, G., Roncoroni, S., Recchia, S., Marchese, L., 2009. On the properties of a novel V-containing saponite catalyst for propene oxidative dehydrogenation. Catal. Lett. 131, 42–48.

Herrero, M., Labajos, F.M., Rives, V., 2009. Size control and optimisation of anionic clays. Appl. Clay Sci. 42, 510–518.

Higashi, S., Miki, H., Komarneni, S., 2007. Mn-smectites: hydrothermal synthesis and characterization. Appl. Clay Sci. 38, 104–112.

Kawi, S., Yao, Z.Y., 1999. Saponite catalysts with systematically varied Mg/Ni ratio: synthesis, characterization, and catalysis. Microporous Mesoporous Mater. 33, 49–59.

Kloprogge, J.T., Breukelaar, J., Jansen, J.B.H., Geus, J.W., 1993. Development of ammonium-saponites from gels with variable ammonium concentration and water-content at low-temperatures. Clays Clay Miner. 41, 103–110.

Kloprogge, J.T., Komarneni, S., Amonette, J.E., 1999. Synthesis of smectite clay minerals: a critical review. Clays Clay Miner. 47, 529–554.

Kloprogge, J.T., Frost, R.L., 2000. The effect of synthesis temperature on the FT-Raman and FT-IR spectra of saponites. Vib. Spectrosc. 23, 119–127.

Kshirsagar, V.S., Garade, A.C., Patil, K.R., Shirai, M., Rode, C.V., 2009a. Liquid Phase Oxidation of p-Cresol over Cobalt Saponite. Top. Catal. 52, 784–788.

Kshirsagar, V.S., Garade, A.C., Patil, K.R., Jha, R.K., Rode, C.V., 2009b. Heterogeneous cobalt-saponite catalyst for liquid phase air oxidation of p-cresol. Ind. Eng. Chem. Res. 48, 9423–9427.

Lowell, S., 1979. Introduction to Powder Surface Area, Willey. Interscience, New York.

Madejová, J., 2003. FT-IR techniques in clay mineral studies. Vib. Spectrosc. 31, 1–10.

Mata, G., Trujillano, R., Vicente, M.A., Korili, S.A., Gil, A., Belver, C., Ciuffi, K.J., Nassar, E.J., Ricci, G.P., Cestari, A., Nakagaki, S., 2009. (Z)-cyclooctene epoxidation and cyclohexane oxidation on Ni/alumina-pillared clay catalysts. Microporous Mesoporous Mater. 124, 218–226.

Polverejan, M., Liu, Y., Pinnavaia, T.J., 2002. Aluminated derivatives of Porous Clay Heterostructures (PCH) assembled from synthetic saponite clay: properties as supermicroporous to small mesoporous acid catalysts. Chem. Mater. 14, 2283–2288.

Prihod'ko, R., Sychev, M., Hensen, E.J.M., van Veen, J.A.R., van Santen, R.A., 2002. Preparation, characterization and catalytic activity of non-hydrothermally synthesized saponite-like materials. Stud. Surf. Sci. Catal. 142, 271–278.

Prihod'ko, R., Hensen, E.J.M., Sychev, M., Stolyarova, I., Shubina, T.E., Astrelin, I., van Santen, R.A., 2004. Physicochemical and catalytic characterization of non-hydrothermally synthesized Mg-, Ni- and Mg–Ni–saponite-like materials. Microporous Mesoporous Mater. 69, 49–63.

Rinaldi, R., Sepulveda, J., Schuchardt, U., 2004. Cyclohexene and cyclooctene epoxidation with aqueous hydrogen peroxide using transition metal-free sol-gel alumina as catalyst. Adv. Synth. Catal. 346, 281–285.

Sivaiah, M.V., Petit, S., Brendlé, J., Patrier, P., 2010. Rapid synthesis of aluminium polycations by microwave assisted hydrolysis of aluminium via decomposition of urea and preparation of Al-pillared montmorillonite. Appl. Clay Sci. 48, 138–145.

Sutton, D., 1970. Electronic Spectra of Transition Metal Complexes. Mc Graw Hill, London.

Trujillano, R., Vicente, M.A., Rives, V., Korili, S.A., Gil, A., Ciuffi, K.J., Nassar, E.J., 2009. Preparation, alumina-pillaring and oxidation catalytic performances of synthetic Ni–saponite. Microporous Mesoporous Mater. 117, 309–316.

Trujillano, R., Rico, E., Vicente, M.A., Herrero, M., Rives, V., 2010. Microwave radiation and mechanical grinding as new ways for preparation of saponite-like materials. Appl. Clay Sci. 48, 32–38.

Vicente, I., Salagre, P., Cesteros, Y., Medina, F., Sueiras, J.E., 2010. Microwave-assisted synthesis of saponite. Appl. Clay Sci. 48, 26–31.

Wells, A.F., 1984. Structural Inorganic Chemistry, 5th edition. Oxford University Press.

Yao, M., Liu, Z.Y., Wang, K.X., Zhu, M.Q., Sun, H.J., 2005. Application of FTIR technique in microwave-hydrothermal synthesis of saponite. Guang Pu Xue Yu Guang Pu Fen Xi 25, 870–873 (Article in Chinese).

Zemanová, M., Link, G., Takayama, S., Nüesch, R., Janek, M., 2006. Modification of layer charge in smectites by microwaves. Appl. Clay Sci. 32, 271–282.

Zhang, D., Zhou, C.-H., Lin, C.-X., Tong, D.-S., Yu, W.-H., 2010. Synthesis of clay minerals. Appl. Clay Sci. 50, 1–11.

Zhou, C.H., 2010. Emerging trends and challenges in synthetic clay-based materials and layered double hydroxides. Appl. Clay Sci. 48, 1–4.